Organic Geochemistry 62 (2013) 46–55

Contents lists available at ScienceDirect

Organic Geochemistry

journal homepage: www.elsevier.com/locate/orggeochem

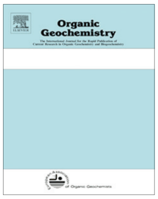

Laboratory charring conditions affect black carbon properties: A case study from Quebec black spruce forests

Laure N. Soucémarianadin [a,*], Sylvie A. Quideau [a], M. Derek MacKenzie [a], Guy M. Bernard [b], Roderick E. Wasylishen [b]

[a] Department of Renewable Resources, University of Alberta, 442 Earth Sciences Building, Edmonton, AB T6G 2E3, Canada
[b] Department of Chemistry – E3-24, Chemistry Centre, University of Alberta, Edmonton, Alberta T6G 2G2, Canada

ARTICLE INFO

Article history:
Received 9 February 2013
Received in revised form 22 June 2013
Accepted 12 July 2013
Available online 21 July 2013

ABSTRACT

Black carbon (BC) is an important residue of wildfires in boreal forests, but its characteristics depend on its formation conditions. The objective of this study was to characterize the chemical and physical properties of BC produced under controlled laboratory conditions, while mimicking a gradient of wildfire severity. We used fuels originating from mosses, ericaceous shrubs and spruce trees, as they constitute the major types available in boreal forests. We varied the maximum temperature (MT) from 75 to 800 °C, the duration of charring from 0.5 to 24 h and the abundance of O_2. BC properties were analyzed using elemental analysis and proximate analysis, solid state ^{13}C nuclear magnetic resonance (NMR) spectroscopy, scanning electron microscopy (SEM) and surface area (SA) analysis. MT was the most significant factor affecting both chemical and physical changes. Results from ^{13}C NMR spectroscopy indicated that 350 °C was a threshold temperature, above which spectra became dominated by aromatic structures for all fuels. Charring duration affected BC composition at both low (250 °C for 12 h vs. 24 h) and high (600 °C for 0.5 h vs. 6 h) MT. The presence of O_2 influenced BC composition mainly at low MT (250 °C) and resulted in accelerated alkyl C degradation, accompanied with a distinct decrease in yield. Results from the SA analysis and the SEM micrographs showed that fuel type influenced BC physical properties, with moss-derived BC presenting higher surface area and microporosity than BC of woody origin.

© 2013 Elsevier Ltd. All rights reserved.

1. Introduction

Black carbon (BC) is commonly defined as the highly condensed carbonaceous residue produced from the incomplete combustion of organic matter (Baldock and Smernik, 2002). Important defining properties are its relative inertness, ubiquity in pyrogenic ecosystems and high content of aromatic structures (Schmidt and Noack, 2000), although BC produced by wildfires tends to be composed of small aromatic clusters (Preston and Schmidt, 2006). However, an ambiguity persists in determining what constitutes BC, as no standard analytical method exists. Masiello (2004) proposed to define it as a continuum. The idea was further explored by Hammes et al. (2007) with an inter-laboratory ring trial that aimed to resolve which techniques best assessed each part of the continuum.

Soil organic carbon (SOC) constitutes by far the most important carbon stock in terrestrial ecosystems. Globally, soils store around 1.5×10^{15} kg C (Schlesinger and Bernhardt, 2013), i.e. 3× the amount above ground in plants and other living organisms. The C reservoir in boreal forest soils is particularly significant; it is estimated at 227×10^{12} kg (Kasischke and Stocks, 2000), which represents 17% of all terrestrial C. Studies have shown that BC may be a significant component of the SOC pool (e.g. Schmidt et al., 1999; Ponomarenko and Anderson, 2001; Skjemstad et al., 2002). Preston and Schmidt (2006) reported BC stocks in boreal forest floor of the order of 1000–2000 kg/ha and considered that this likely underestimated the real stocks. Indeed, in boreal forests, the combustion of the thick forest floor layers by wildfire is often incomplete and BC is a major outcome.

In addition to its potential importance in contributing to the overall SOC pool, the amount of BC left on site after fire may affect ecosystem recovery through modification of plant community dynamics and by stimulation of the N cycle (DeLuca et al., 2006). BC plays a notable role in soil microbial activity and nutrient cycling after fire (Wardle et al., 1998; DeLuca et al., 2006). Unfortunately, there is a lack of knowledge with regard to its composition and morphological features, although these may contribute to the rejuvenating effect of wildfire on soil properties (Certini, 2005). For instance, porosity directly affects the role BC plays in retaining water, nutrients and/or tannins, and its potential to provide habitats for microorganisms (Hockaday et al., 2006, 2007; Zackrisson et al., 1996). Characterization of BC chemical and physical properties is, moreover, critical for its quantification, as demonstrated by, e.g., Hammes et al. (2007) and Keiluweit et al. (2010). At the same time, there is an immediate need to introduce the BC pool into global carbon models under future climate change

---

* Corresponding author. Tel.: +1 780 492 2115; fax: +1 780 492 1767.
E-mail address: soucmari@ualberta.ca (L.N. Soucémarianadin).

0146-6380/$ - see front matter © 2013 Elsevier Ltd. All rights reserved.
http://dx.doi.org/10.1016/j.orggeochem.2013.07.005

conditions (Bergeron and Flannigan, 1995), especially since an increase in fire frequency is expected for the boreal region.

In this study, we focussed on BC properties that directly affect its ability to impact on soil functioning after fire, including its elemental and macromolecular composition, and several key physical characteristics, such as porosity and surface area. We produced BC samples under controlled conditions and analyzed them using a set of diverse methods to (i) identify the range of chemical and physical properties of BC as it might be produced in boreal forests and (ii) identify the different influences of the formation conditions on these properties under a range of fire severity. The study is unique in its attempt to investigate the effect of thermal treatment simulating different wildfire conditions on major fuels from boreal forests.

2. Material and methods

2.1. Reference set

We created a reference set of laboratory-produced BC samples ($n = 88$) by controlling several key variables, namely: type of fuel (Hammes et al., 2006), maximum temperature reached during combustion (Baldock and Smernik, 2002; Brown et al., 2006) and duration of charring (Baldock and Smernik, 2002). We also explored the influence of the abundance of O_2 available during the thermal treatment on BC chemical properties.

We selected biomass representing the most common fuels available in Quebec black spruce–moss forests. These included fresh (L) and partially humified (F) layers of *Sphagnum* spp. and *Pleurozium shreberi* dominated forest floor, bark, branches and needles from black spruce (*Picea mariana*), cones, branches and needles from jack pine (*Pinus banksiana* Lamb.) and twigs and leaves from Labrador tea (*Rhododendron groenlandicum*). Similar fuel types are available in many boreal forests throughout Eurasia and North America.

2.2. Charring conditions

We chose the temperature and duration of charring associated with each charcoalification (Orvis et al., 2005) experiment to mimic, as closely as possible, a range of plausible wildfire conditions, as they might occur in boreal forests (Miyanishi, 2001; Ryan, 2002; Taylor et al., 2004; Rein et al., 2008). Specifically, we varied the maximum temperature (MT) from 75 to 800 °C and the duration of charring from 0.5 to 24 h. We paired the charring conditions (MT, duration and O_2) to further analyze their influence (Table A.1). The experiments were performed with a muffle furnace under controlled temperature and charring duration. The amount of O_2 was varied by either placing the fuels in a tin with a cap pierced with tiny holes (limited O_2 input, i.e. partial pyrolysis) or by tightly wrapping them in Al foil before putting them in a sand bath (full pyrolysis). The objective of this O_2 treatment was to simulate variation in pyrolysis conditions as they are likely to occur during a wildfire [BC forms both during the flaming and smoldering stages (Schmidt and Noack, 2000)]. However, the experimental set-up did not allow us to measure differences in O_2 content between the SB and T experiments. Charring duration refers to the time during which the fuel was held at MT. The time taken to reach MT was not included as one of the variables, and total time in the furnace varied among charcoalification experiments. The higher MTs ($\geqslant$ 600 °C) were associated with short charring duration (Table A.1) as, during a wildfire, these temperatures are not likely to persist for long periods of time. With the muffle furnace, there was no possible adjustment of the heating rate. However, the latter was recorded and proved to be relatively constant among the different batches (13–19 °C min^{-1}), so we considered it a fixed parameter. Sufficient amount of fuel was used for each BC production to give at least 4 g of BC sample.

2.3. BC characterization

The BC samples were finely ground using a mortar and pestle or a mortar grinder (RM 100 mortar grinder, Retsch, Haan, Germany). The total amounts of C, H and N were determined from dry combustion using a CHN Analyzer (CEC – Control Equipment Corporation – Model 440 Elemental Analyzer with auto-injector). O content was estimated by difference from the ash free mass of the sample obtained after 6 h at 750 °C in a muffle furnace, in accord with ASTM Standard D1762-84 (ASTM, 2007). The procedure also provided the total ash content. All results reported for C, H, N and O were normalized to a dry and ash-free basis.

Physical properties were characterized as follows. The BET (Brunauer et al., 1938) specific surface area (multipoint) and the pore size distribution were characterised from N adsorption and desorption isotherms measured at 77.3 K with an Autosorb 1MP surface area analyzer (Quantachrome Instruments Corp., Boynton Beach, FL). Prior to analysis, samples were degassed at room temperature up to 150 °C (depending on the MT of formation) for 3–27 h (average degassing time 20 h). BET surface area was derived from a multipoint plot over a range of relative pressure, $P/P_o = 0.05–0.35$ (Sing et al., 1985). Calculation of the different pore volumes was done using the pore volume data with Autosorb 1 for Windows 1.52.

BC heterogeneity, notably the size and shape of pores, was assessed using scanning electron microscopy (SEM). High resolution digital images of the surface of different BC samples were obtained using a field emission SEM instrument (JEOL 6301F – JEOL Ltd.) with magnification ranging from 20× to 50,000×. Before being imaged through the SEM instrument, samples were coated with Au (Nanotech SEMPrep 2 sputter coater) to increase conductivity.

2.4. Spectroscopic analysis

To characterize BC macromolecular structure, we used a nondestructive method: solid-state ^{13}C NMR spectroscopy with magic angle spinning (MAS). The ^{13}C nuclei (1.1% natural abundance) provide information about the various functional groups in samples (Axelson, 2012). Usually studies focussing on organic matter use cross polarization (CP) as it generally allows acquisition of ^{13}C NMR spectra in less time. However, the CP efficiency for chars is reduced (Baldock and Smernik, 2002) because of the absence of particularly mobile ^{1}H nuclei (Freitas et al., 1999; Smernik et al., 2002). To verify that our CP spectra were representative we used the more quantitative Bloch decay (BD), also called direct polarisation (DP), technique (Preston and Schmidt, 2006) on a subset of samples.

^{13}C NMR was conducted with a Chemagnetics CMX Infinity 200 Spectrometer. A 7.5 mm Chemagnetics double resonance MAS probe was used to spin the samples at 5 kHz at the magic angle (54.7°). Samples were packed into a 7.5 mm o.d. zirconium oxide rotor equipped with a Kel-F® drive tip and Teflon end cap and spacer. Chemical shifts (ppm) were externally referenced to tetramethylsilane (TMS) by setting the high frequency peak for adamantane to 38.56 ppm (Earl and VanderHart, 1982). Spectra were acquired at 50.3 MHz.

We used a variable-amplitude CP (VACP) pulse sequence (Peersen et al., 1993) to obtain the free induction decays (FIDs) of the CP spectra, using a spectral width of 30 kHz; 1024 data points were collected over an acquisition time of 34.1 ms. All spectra were then zero-filled to 8192 data points. The background ^{13}C NMR signal, obtained by acquisition of the spectrum from an empty rotor, was subtracted before processing the FIDs. The number of scans acquired for the CP spectra ranged from 8432 to 9468. We used a 1 ms contact time, 90° ^{1}H pulse of 4.5 μs duration and recycle delay of 10 s. Finally, we applied Lorentzian line broadening of 60–100 Hz before performing the Fourier Transform. The spectra were divided into eight spectral regions, each corresponding to a major C type, as described by Baldock and Smernik (2002). Briefly, the intensity associated with the following regions was quantified by integration: ketone C (215–190 ppm), carbonyl and amide C (190–165 ppm), O-aryl C (165–145 ppm), aryl and unsaturated C (145–110 ppm), di-O-alkyl C (110–90 ppm), O-alkyl C (90–65 ppm), methoxyl and N-alkyl C (65–45 ppm), alkyl C (45–0 ppm), while using the regions with high chemical shift (290–215 ppm) to correct for the spinning side bands. In doing so, we assumed that the side bands were of equal intensity on either side of the isotropic peak. While likely accurate for the aromatics, this may not be so true for carbonyls. Because our spectra did not show any large carbonyl peak, we decided that it was safe to apply this methodology. For part of the statistical analysis, the regions were simplified into four regions: carbonyl C (215–165 ppm); aromatic and phenolic C (165–110 ppm); O-alkyl C (110–45 ppm); alkyl C (45–0 ppm).

For the DP spectra, 884–888 scans were acquired using a 90° ^{13}C pulse of 4.5 μs. To allow complete relaxation, the recycle delay was set to 100 s. The FID of the background signal was subtracted from the FID of the sample before processing; all spectra were zero-filled to 8192 data points and a Lorentzian line broadening of 60–100 Hz was applied to the FID. Applying Smernik and Oades' (2000a) methodology, we used spin counting to determine if the DP spectra were representative of all the C moieties in the samples. Glycine (Fisher Scientific, reagent grade) was used as external reference material. The C observability, C_{obs}, corresponds to the fraction of the expected NMR intensity actually observed. It is assumed that the intensity of the NMR resonances quantitatively reflects the distribution of ^{13}C environments in the sample if $C_{obs} = 100\%$ (Smernik and Oades, 2000b). A value < 100% implies that part of the potential signal was not detected.

Even though CP experiments are not commonly considered as quantitative, we concluded, based on comparison with the respective DP spectra, that they represented the distribution of the total intensity quite accurately, further indicating that the majority of the aromatic/quaternary carbons were efficiently cross-polarized. The results (Table B.1) are similar to previous observations (Baldock and Smernik, 2002; Knicker et al., 2005). We therefore used the results from the VACP spectra for the remainder of the study.

2.5. Data analysis

The analytical methods were applied to different subsets of samples in order to reduce the cost and time of analysis. Elemental analysis was performed on 67 of the 88 samples. The ^{13}C NMR

Table 1
Yield (%) and characteristics of BC produced from three fuel types [*Sphagnum* spp., black spruce (BSP) branch and *Rhododendron g.*], under varying maximum temperature (MT), charring duration and pyrolysis type [sand bath (SB) without O_2; tin (T) with limited O_2; nd, not determined].

Fuel	MT (°C)	Charring duration (h)	Pyrolysis type	Yield[a] (%)	Moisture content (%)	Ash content (%)	C[b,c] (%)	H[b,c] (%)	N[b,c] (%)	O[b] (%)	C/N	Atomic H/C[b]	Atomic O/C[b]	Specific SA (multipoint BET – m^2/g)	Degree of aromatisation[d]
Sphagnum	75	24	SB	99.4	7.3	1.55	46.49 (0.67)	5.66 (0.09)	0.61 (0.01)	47.24	76.3	1.46	0.76	2.5	0.41
Sphagnum	250	24	SB	53.4	2.5	6.17	70.49	4.25	1.43	23.83	49.2	0.72	0.25	nd	1.78
Sphagnum	350	12	SB	41.5	1.2	9.02	70.87	4.07	1.45	23.62	48.9	0.69	0.25	13.8	3.27
Sphagnum	425	6	SB	31.5	6.2	8.87	74.20	2.77	1.59	21.45	46.7	0.45	0.22	231.1	5.59
Sphagnum	600	0.5	T	27.7	1.3	5.02	88.02 (0.30)	2.52 (0.31)	1.14 (0.05)	8.32	77.3	0.34	0.07	315.0	21.51
Sphagnum	600	0.5	SB	30.3	1.0	7.61	86.21	2.85	1.27	9.67	67.9	0.40	0.08	nd	8.59
Sphagnum	800	0.5	SB	18.3	2.5	26.98	84.27 (5.44)	1.35 (0.08)	1.13 (0.04)	13.25	74.6	0.19	0.12	502.9	nd
BSP branch	75	24	SB	100.2	4.6	1.02	49.52 (1.41)	5.80 (0.25)	0.51 (0.10)	44.17	98.0	1.41	0.67	2.2	0.23
BSP branch	250	24	SB	63.5	2.1	1.41	64.08 (1.58)	5.08 (0.22)	0.50 (0.11)	30.34	129.0	0.95	0.36	0.6	0.74
BSP branch	350	12	SB	40.1	0.8	2.73	77.35	4.16	0.72	17.77	107.6	0.65	0.17	5.2	2.65
BSP branch	425	6	SB	30.6	2.9	3.22	76.20 (8.03)	3.10 (0.53)	0.57 (0.20)	20.13	133.0	0.49	0.20	18.3	10.57
BSP branch	600	0.5	SB	28.2	2.6	3.30	72.88 (10.56)	2.93 (0.77)	0.53 (0.14)	23.66	137.0	0.48	0.24	89.5	5.91
BSP branch	800	0.5	SB	23.0	2.6	7.82	89.92 (0.58)	1.47 (0.05)	0.82 (0.01)	7.78	109.0	0.20	0.06	365.7	nd
Rhododendron	75	24	SB	100.3	4.6	2.28	53.51 (0.09)	6.50 (0.07)	1.65 (0.07)	38.34	32.5	1.46	0.54	nd	0.39
Rhododendron	250	24	SB	62.1	1.4	3.74	66.24 (1.58)	4.64 (0.22)	2.31 (0.10)	26.81	28.7	0.84	0.30	1.0	0.90
Rhododendron	350	12	SB	41.4	2.0	5.45	77.81 (0.13)	4.49 (0.04)	2.03 (0.01)	15.66	38.3	0.69	0.15	12.8	2.53
Rhododendron	425	6	SB	32.6	0.6	6.23	77.46 (3.28)	3.32 (0.38)	2.55 (0.33)	16.66	30.4	0.52	0.16	3.7	11.33
Rhododendron	600	0.5	SB	30.5	1.0	6.85	72.30 (12.61)	3.11 (0.36)	2.35 (0.44)	22.23	30.7	0.52	0.23	nd	8.52
Rhododendron	800	0.5	SB	22.3	6.8	18.44	82.46 (0.17)	1.37 (0.00)	1.62 (0.03)	14.54	50.8	0.20	0.13	nd	nd

[a] Dry wt. basis.
[b] Dry wt. and ash-free basis.
[c] Average (± SD), *n* = 3.
[d] Degree of aromatisation defined by aromatic C/(aliphatic + O-containing C) ratio from ^{13}C NMR CP spectra (i.e. ratio of the [165–110 ppm]/[110–0 ppm] regions).

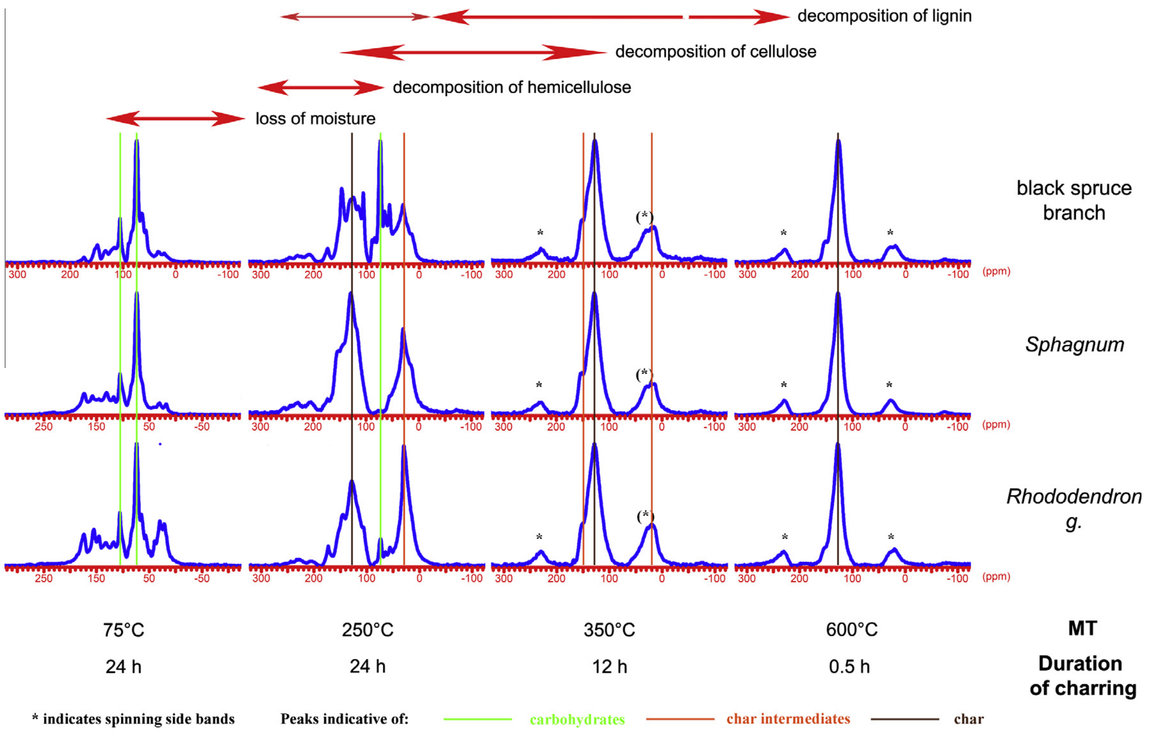

Fig. 1. ^{13}C VACP NMR spectra of black spruce branch, *Sphagnum* and *Rhododendron*, submitted to different maximum temperature (MT) and charring duration.

VACP experiment was performed on 40 samples [*Sphagnum* spp.; black spruce (bark; branches + twigs; needles); *Rhododendron g.*], while only a subset of ten BC samples was subjected to both VACP and DP associated with spin counting ^{13}C NMR experiments. We were not able to acquire ^{13}C NMR spectra for the BC produced at 800 °C because of our inability to properly tune the probe containing these samples. This phenomenon has been related to the high electrical conductivity associated with the alignment of aromatic sheets (Freitas et al., 1999) in such samples. Because surface area analysis is time consuming, only a subset of 14 samples (*Sphagnum*; black spruce branch; *Rhododendron g.* at specific MTs) was examined. Finally, SEM micrographs were obtained for 20 samples [*Sphagnum* spp.; black spruce (branch + bark); *Rhododendron g.* at specific MTs].

The different biomass types were grouped into the following four main fuel types for part of the statistical analysis: moss (*Sphagnum* spp. and *P. shreberi*), ericaceous shrub (*Rhododendron g.*), "wood" (branches and bark) and needles from black spruce (*P. mariana*).

We conducted analysis of variance (one way and two ways) and paired *t*-tests to isolate the influence of the different formation factors, using SAS 9.2 (SAS Institute Inc., Cary, North Carolina). The influence of duration of charring and O_2 abundance on BC physical properties was not tested because of time limitations; for these two variables, the results below only cover chemical properties.

3. Results and discussion

3.1. Influence of MT

3.1.1. Yield and chemical composition

The yield of BC decreased with increasing MT (Table 1). Most of the distinct decrease (36–50%) between 75 °C and 250 °C could be attributed to moisture loss (Melkior et al., 2012). There was another steep decrease between 250 °C and 350 °C, likely due to the decomposition of hemicellulose and release of CO and CO_2 (Miyanishi, 2001). The remaining yield decrease for MT $\geqslant$ 350 °C could be explained by cellulose degradation followed by lignin degradation (Antal and Grønli, 2003; Belderok, 2007; Melkior et al., 2012). The additional weight loss > 425 °C was smaller (5–13% decrease) and likely caused by the final stages of lignin degradation and release of volatile matter (including tar).

For all fuel types, we observed a progressive increase in C content and a decrease in O and H contents with increasing MT (Table 1). The atomic H/C ratio values generally agreed with observations from Hammes et al. (2006), who reported that an atomic H/C ratio > 0.5 seemed to characterize chars which experienced temperatures < 500 °C, whereas chars with H/C < 0.5 were mostly formed at higher temperature ($\geqslant$500 °C). For all fuels, N concentration first slightly increased up to 425 °C and then decreased back to initial level (Table 1). The trend agrees with previous studies (Baldock and Smernik, 2002; Lang et al., 2005; Calvelo Pereira et al., 2011) and suggests that at low to intermediate temperature ($\leqslant$ 425 °C), N is included in newly formed unsaturated heterocyclic compounds (Knicker, 2007) and is not volatilized until higher temperature. The BC ash content also increased with increasing MT and BC produced at 800 °C contained significantly more ash than BC formed at lower MT (Table 1).

For temperatures as low as 250 °C, a change in the NMR spectra was observed for all fuels (Fig. 1), with a relative decrease in the signals characteristic of carbohydrates (105 ppm, 74 ppm, etc.) compared with the materials treated at 75 °C. As MT increased from 250 to 350 °C, there was a shift from BC spectra dominated by O-alkyl functional groups (related to cellulose and hemicelluloses) to aryl and alkyl dominated spectra. The NMR spectra confirmed results from the elemental analysis in that the transition between 250 and 350 °C was a key point for the evolution of the samples along the temperature gradient. At 350 °C, the relative increase and appearance of broad peaks around 130 ppm and 20–25 ppm matched the beginning of char formation (Inari et al., 2007).

The distinct shoulder around 150 ppm in spectra from MT $\geqslant$ 250 °C is due to aromatic C linked to O, such as in phenols and derivatives (Freitas et al., 1999). Above 350 °C, the ^{13}C NMR

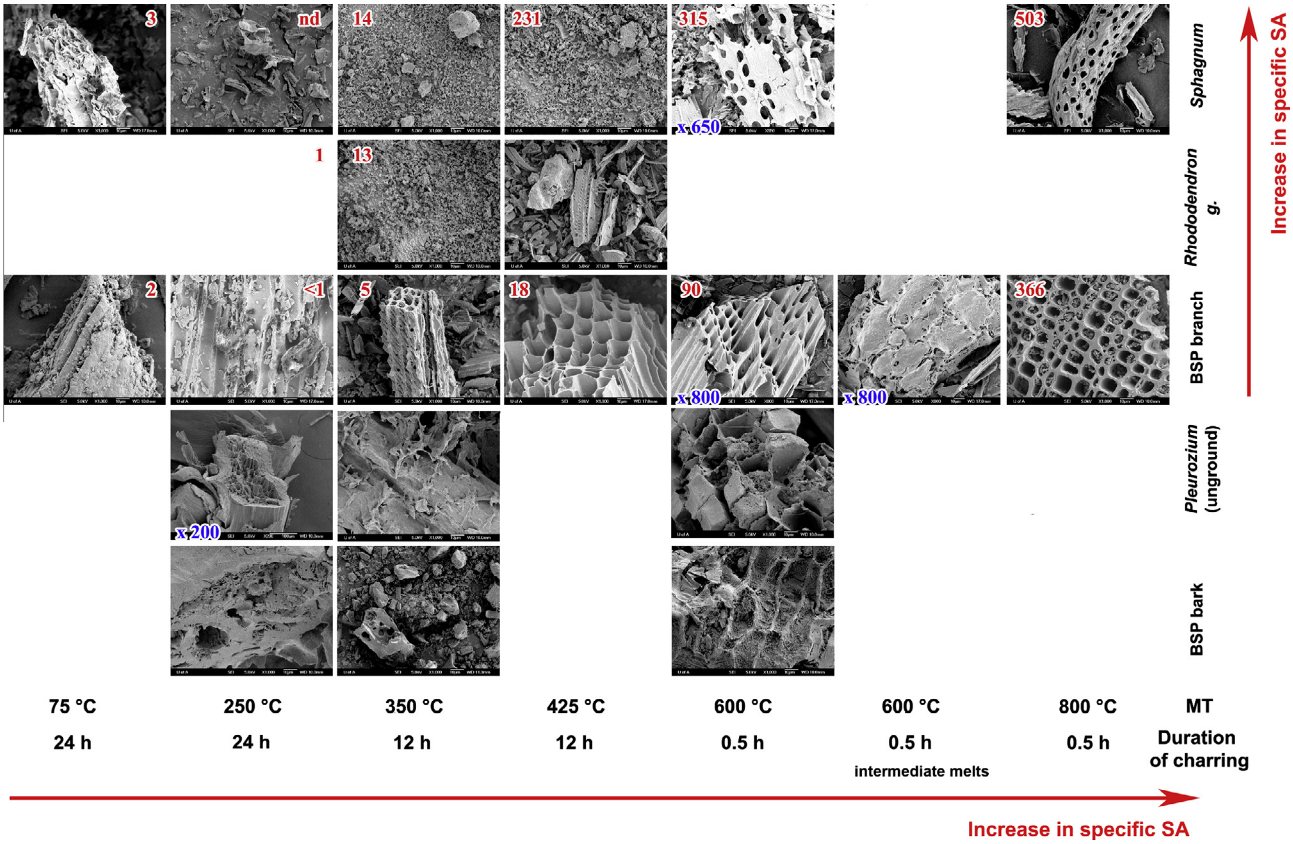

Fig. 2. SEM micrographs of BC from black spruce (BSP) wood (bark and branches), *Sphagnum* and *Rhododendron* submitted to increasing MT. The associated duration of charring is indicated. Magnification is 1000× unless otherwise specified. Specific surface area (SA) in $m^2\ g^{-1}$ obtained from N_2 BET multipoint is also shown.

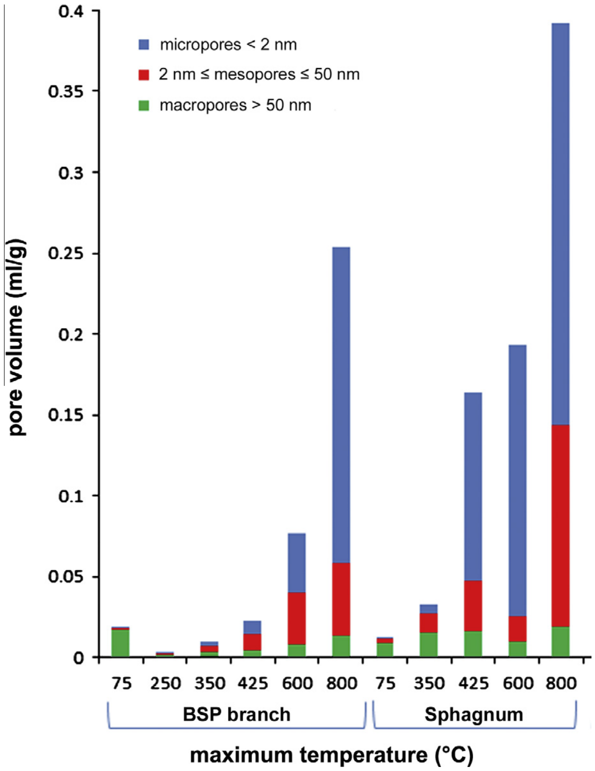

Fig. 3. Distribution of total pore volume (ml/g) between micro, meso and macropores for BC produced from black spruce (BSP) branch and *Sphagnum* at various MT values.

spectra were dominated by aromatic non-oxygenated carbons (130 ppm), the latter peak becoming narrower with increasing MT.

The dominance of aryl groups with increasing MT (Fig. 1) reflected the conversion of macromolecules to small aromatic O-containing heterocyclics (Baldock and Smernik, 2002; Chatterjee et al., 2012). Using the spectroscopic data, we calculated the degree of aromatisation, which corresponds to the ratio of aromatic C (165–110 ppm) to aliphatic and O-containing C (110–0 ppm) (Keiluweit et al., 2010). When comparing BC formed under strictly pyrolytic conditions (SB), the degree of aromatisation significantly increased with increasing MT, corresponding to decreasing H/C and O/C atomic ratios (Table 1). This increase in the relative proportion of aryl-C structures is an indicator of the increasingly condensed nature of chars (Keiluweit et al., 2010). At 800 °C, the formation of structures containing unsaturated carbons, such as aromatic rings associated with the increase in condensation, was indirectly noticeable by our inability to properly tune the probe containing BC formed at this MT, as reported by Freitas et al. (1999).

The increase in aromatic content and decrease in atomic ratios observed with increasing MT have been associated with increasing resistance to biotic degradation (e.g. Baldock and Smernik, 2002; Zimmerman, 2010; Harvey et al., 2012). This is an important result regarding BC potential as a valuable carbon sink after wildfires.

3.1.2. Physical properties

With increasing temperature, we observed an increase in specific surface area (by two orders of magnitude between 75 °C and 600 °C) for the black spruce and the *Sphagnum* BC (Table 1). Similar observations were made by Hammes et al. (2006) in an investigation of grass and wood chars. From comparison with other BC studies, they deduced that BC formed at low temperature tends to have

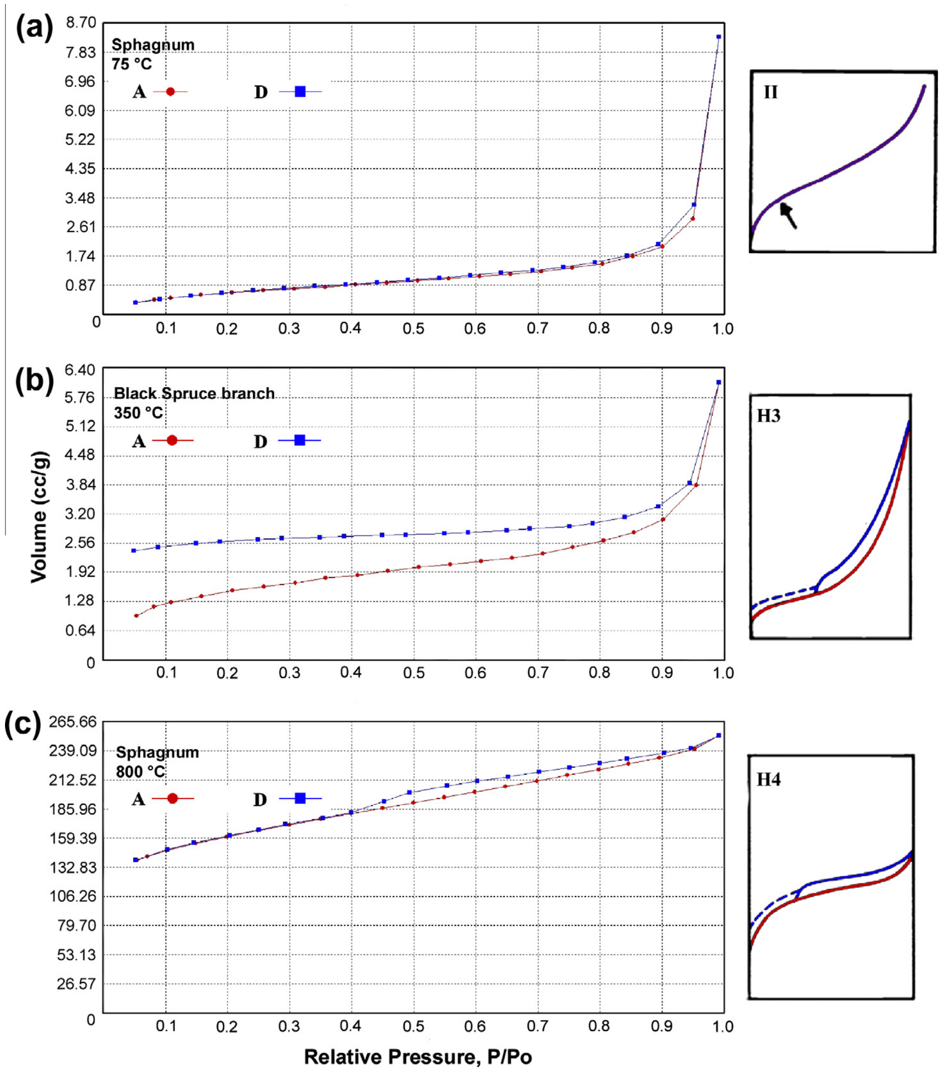

Fig. 4. Main types of physisorption isotherms and hysteresis loops: (a) BC from *Sphagnum* at 75 °C, with a type II isotherm; (b) BC from black spruce branch at 350 °C, with a type H3 hysteresis loop (indicative of narrow slit-shaped pores); (c) BC from *Sphagnum* at 800 °C, with a type H4 hysteresis loop (indicative of micropores). A, adsorption; D, desorption. The inserts on the right are ideal representations of types of physisorption isotherms or types of hysteresis loops.

low surface area (< 25 $m^2\ g^{-1}$), while BC formed at high temperatures usually has a large surface area (214–336 $m^2\ g^{-1}$). As illustrated from SEM, samples produced at 75 °C and 250 °C showed little porosity (Fig. 2). In these samples, cell structures were also preserved, with the membrane of the bordered pits clearly present for the *Rhododendron* and black spruce branch BC. The largest increase in specific SA (both for black spruce branch and *Sphagnum*) occurred between 600 °C and 800 °C, and was particularly marked for the wood BC (Table 1). With this range of MT, we also observed a partial or total destruction of fuel cell structure (Fig. 2). At 600 °C, there was evidence of intermediate melt in the structure of BC from black spruce branch. This was likely formed by the decomposition and softening of some volatile fractions (Lua et al., 2004), which could explain the relatively lower BET surface area vs. the BC from *Sphagnum* (Table 1).

The increase in MT resulted in changes in the distribution of BC porosity (Fig. 3). The shape of the adsorption and desorption isotherms and their associated hysteresis loops (Fig. 4) also helped characterize the type and shape of the pores (Han et al., 2006). Type II isotherms with a very small closed hysteresis loop (Fig. 4a) included BC from *Sphagnum* at 75 °C, black spruce branch at 75 °C and 250 °C and *Rhododendron* at 250 °C), and was characteristic of a porosity dominated by macropores (Fig. 3). BC from *Rhododendron* at 425 °C, black spruce branch, *Sphagnum* and *Rhododendron* at 350 °C engendered a type H3 non-closed hysteresis loop (Fig. 4b), indicative of narrow slit-shaped pores (Bourke et al., 2007). Finally, BC from black spruce branch and *Sphagnum* at 425 °C and 600 °C, and black spruce branch and *Sphagnum* at 800 °C generated a type H4 hysteresis loop. The 800 °C, BC had a closed loop (Fig. 4c), while BC formed at lower temperatures presented a non-closed loop. Slit-like pores are frequently the cause of a type H4 hysteresis loop, and these samples, exhibiting the highest measured specific surface areas, were dominated by micropores (Fig. 3). In a review including studies of BC produced under controlled conditions from various fuels and at a broad range of temperature, Downie et al. (2009) similarly reported an increase in specific SA, related mostly to an increase in microporosity with high MT.

3.2. *Influence of fuel type*

3.2.1. *Yield and chemical composition*

There were no significant differences in BC yield between the various types of fuel when considering the entire temperature gradient, and comparing analogous charring conditions (Table 1). Similarly, atomic ratios and C content were not significantly influenced

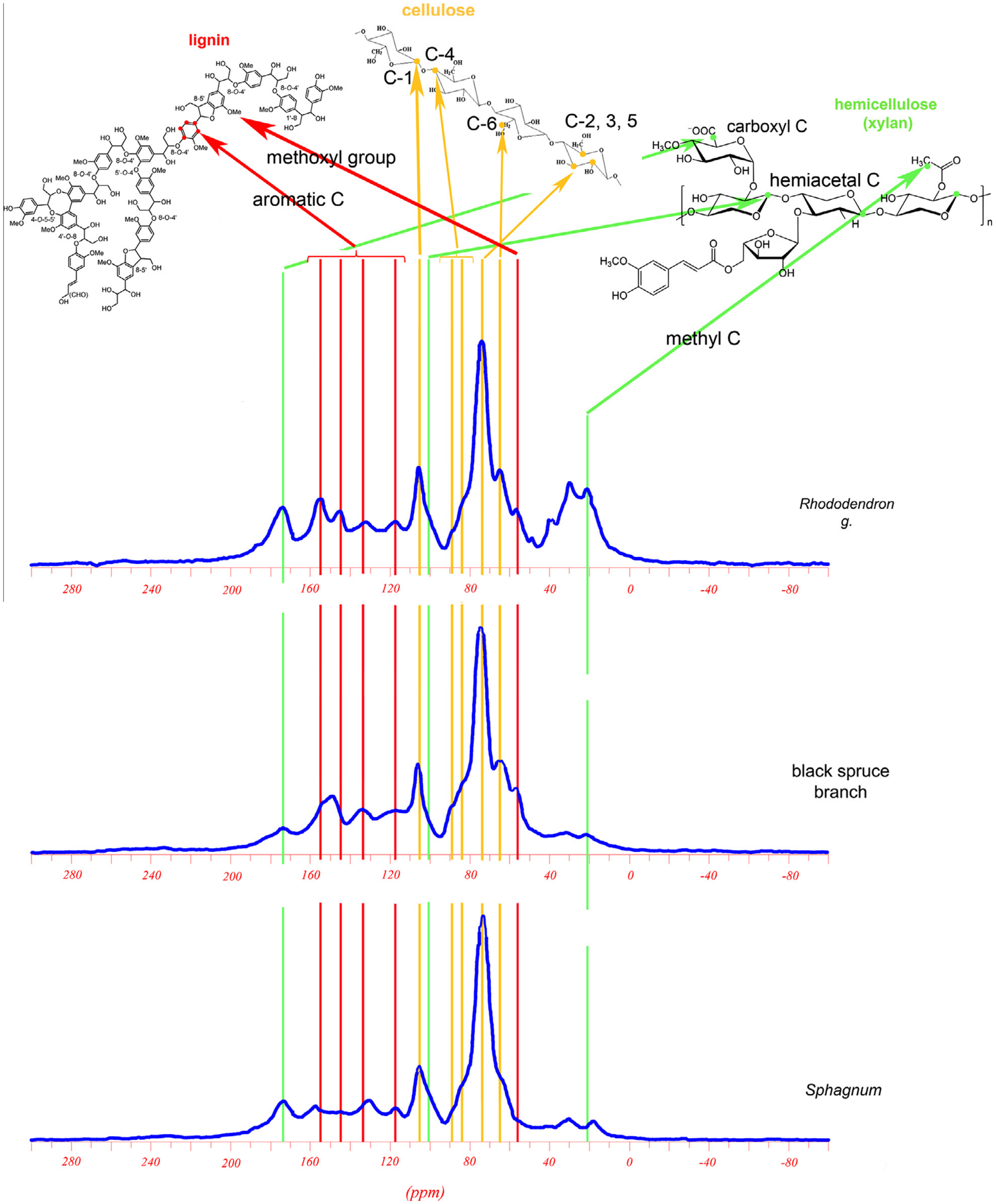

Fig. 5. ^{13}C CP NMR spectra of three fuels after a thermal treatment at 75 °C for 24 h. Functional groups of the constituent macromolecules (cellulose, hemicelluloses and lignin) are tentatively assigned to the main peaks.

by the type of fuel. BC from black spruce branches generated less ash than the BC from other precursor materials. This could be explained by the fact that the non-photosynthetic parts of softwood trees have a relatively low ash content vs. other fuels (Ponomarenko and Anderson, 2001). However, there was no significant difference in ash content over the whole thermal gradient between the various types of fuel.

The ^{13}C NMR spectra illustrate how fuel type affected the composition of the samples exposed to low thermal treatment (Fig. 5). When only dried (75 °C), the different types of fuel gave distinctive spectra exhibiting representative peaks attributed to cellulose, hemicelluloses and lignin (Wikberg and Maunu, 2004; Inari et al., 2007; Melkior et al., 2012). Based on the relative intensity of the different peaks in the *Sphagnum* spectrum (Fig. 5), it could be concluded that this particular fuel contained a higher proportion of carbohydrates than the black spruce wood or the ericaceous shrub. This can be explained by the reduced lignin fraction in this particular fuel type.

Differences among fuel types persisted until a MT of 250–350 °C (Fig. 1). At 250 °C, the spectrum of black spruce BC looked far more complex than the one from *Rhododendron* or *Sphagnum*. For all fuels, there was a distinct increase in the aromatic and phenolic C content, compared with results from 75 °C. The black spruce and *Rhododendron* had a smaller increase in carbonyl C. The appearance of a broad peak centered around 20–25 ppm for all fuels indicated a higher alkyl content. This signal was most intense for *Rhododendron* and also sharper, suggesting less heterogeneity in the functional groups present. Peaks at 65, 74, 84 and 89 ppm in the black spruce BC clearly revealed the persistence of the cellulose. Peaks related to cellulose decreased substantially for the *Rhododendron* and were totally absent from the *Sphagnum* BC spectrum (Fig. 1). Hemicellulose (173 ppm) and lignin (56 ppm) structures were still visible in the black spruce and *Rhododendron* BC spectra. The near disappearance of the other hemicellulose signals (20 ppm and 102 ppm), paralleled by the increase in relative intensity of the peak at 173 ppm, suggested carbohydrate degradation with concurrent acetic acid release (Sivonen et al., 2005).

At 350 °C, the spectra began to look similar for all fuels, with the broad peak in the aromatic and phenolic C region (130 ppm) becoming predominant (Fig. 1). The BC from *Sphagnum* differed from BC produced from other fuels, with significant char formation that began at lower temperature (250 °C) than for the two other precursor materials (around 350 °C). Once again, this could be related to the reduced amount of the more thermally resistant lignin fraction. This result is important since this type of fuel represents a large C input to black spruce ecosystems, as shown by Harden et al. (1997, 2000) and Yu et al. (2002). For MT > 350 °C, there was no difference in the composition of BC produced from the different fuels. This is a slightly lower MT than that reported by Krull et al. (2009) in their review (500–600 °C), but the difference could be a result of the different duration of charring in the various studies.

3.2.2. Physical properties

Here we focus on the differences and/or changes in physical properties that are fuel-specific. We observed large differences in BC specific surface area produced from the different feedstocks (Table 1). Considering analogous thermal treatments (MT, duration of charring, O_2 abundance), the black spruce wood led to BC with a smaller specific surface area than the one created from the ericaceous shrub, which in turn had a smaller specific SA than that of *Sphagnum* origin. BC from wood usually had higher SA than BC of grass origin (e.g. Keiluweit et al., 2010), as the original vascular structure and the pores created by escaping gas combined to produce a porous BC. On the SEM micrographs, the carbonaceous skeleton of the former wood capillary structure was clearly visible (pores in the range of 10 μm) for the black spruce wood BC produced at high MT (Fig. 2). The higher values for the *Sphagnum* BC might be more related to the higher proportion of very small and rough particles in these samples rather than actual porosity. Pore volume distribution was also influenced by fuel type (Fig. 3), with a higher proportion of micropores in the BC from *Sphagnum*. Based on the importance of moss in boreal forests, the distinctive physical characteristics of moss BC are likely to be important for post-fire forest floor properties.

3.3. Influence of charring duration

Overall BC yield did not appear to be affected by the differences in charring duration. Lua et al. (2004) reported similar results and observed that, once charring exceeded 2 h, the yield did not decrease further. Duration of charring only appeared to significantly influence the H/C ratio for the 600 °C charcoalification experiment. Shorter exposure (0.5 h vs. 6 h) did not influence the O/C atomic ratio, but resulted in higher H/C atomic ratio (Fig. 6). Although there was no significant difference, BC produced with longer exposure to the MT had a higher ash content than BC exposed for shorter time. The evolution of the atomic ratios between the BC formed at 600 °C for 6 h with the BC formed at 800 °C for 0.5 h indicates that dehydrogenation was the only reaction occurring for the latter (Fig. 6). On the other hand, the main reactions between 600 °C and 800 °C, when the charring duration was kept at 0.5 h for both MTs, followed a condensation pathway.

The trend in the evolution of the atomic ratios with increasing MT (Fig. 6) is the same as that observed in two independent studies (Baldock and Smernik, 2002; Keiluweit et al., 2010); however there are some differences worthy of discussion. The atomic ratios for our samples differed from those of Baldock and Smernik (2002) and Keiluweit et al. (2010), especially at low and intermediate temperatures (Fig. 6). The main difference between the formation conditions of all the BC samples was the duration of charring: 1 h for Keiluweit et al. (2010), 24–72 h (until BC reached a constant mass) for Baldock and Smernik (2002) and 0.5–24 h in our study. Charring duration is likely responsible for the discrepancy in atomic ratio values; our results are indeed much closer to those obtained by Baldock and Smernik (2002), as were the charring durations we used.

3.4. Influence of oxygen

The presence of O_2 significantly decreased BC yield at 250 °C. At the other MT, yield of BC produced in a tin or sand bath was not significantly different (data not shown). This can be explained by the fact that O_2 favours more complete combustion, reducing the production of char while producing more gas; this is exacerbated

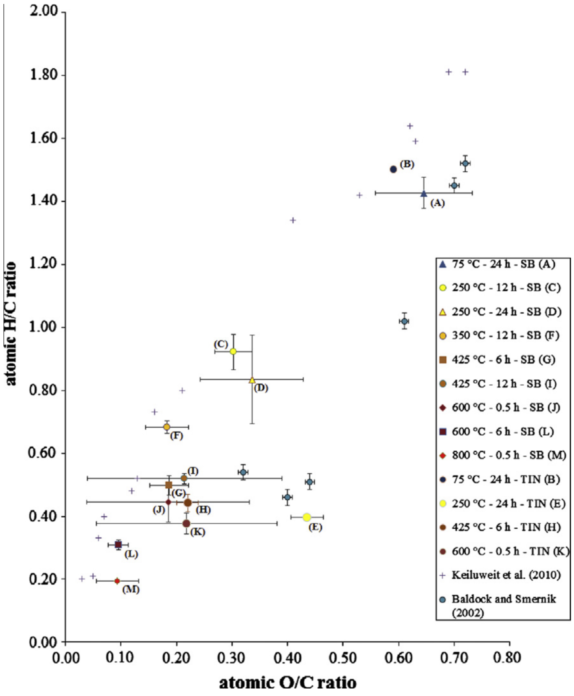

Fig. 6. Van Krevelen diagram showing BC produced here and BC from Keiluweit et al. (2010) and Baldock and Smernik (2002). Our BC produced in full (SB) and partial (TIN) pyrolysis conditions is reported. Values represent an average (± standard deviation) for a given MT and duration of charring.

at lower temperature. CO_2 is indeed one of the most abundant gaseous products at the early stages of combustion (Degroot et al., 1988; Behar and Hatcher, 1995).

BC samples produced in tins (with O_2) at low temperature appeared as outliers from the main trend for a given fuel (Fig. 6). At 250 °C, the presence of O_2 gave BC with significantly lower H/C values (2–3×) than those of BC produced under fully anoxic conditions (Fig. 6). On the other hand, the influence of O_2 on BC produced at higher temperatures was minimal (Fig. 6). Further, its presence did not appear to significantly alter the O/C ratio, or the N content or ash content. The latter was unexpected, as a more efficient charring process (in the presence of O_2) should have increased the ash content of the residue (Krull et al., 2009). This might be related to the MT as well as the duration of charring. During thermal treatment, the fuel experienced two of the three following processes: drying (up to 150 °C); pyrolysis (in the absence of O_2); and oxidation (when O_2 was present). Under total pyrolysis conditions, condensation was the main pathway along the increasing thermal treatment gradient, whereas when O_2 was at least partially available, oxidation prevailed (Fig. 6).

3.5. Relative importance of various formation factors – example of the degree of aromatisation

The degree of aromatisation illustrates the relative influence of the various formation factors (Fig. 7). When there was only dehydration (75 °C; 24 h), the degree of aromatisation was very low under both conditions of pyrolysis (with or without O_2). It increased for BC produced at 250 °C (24 h). At that temperature, the presence of O_2 greatly favoured condensation (5-fold). If one compares the atomic O/C ratio and H/C ratio for these samples (Fig. 6), in the presence of O_2, our values were close to those obtained by Baldock and Smernik (2002), implying that maximum condensation had been reached. Similarly, increasing the duration of charring from 12 to 24 h allowed greater condensation, as shown by the decrease in H/C ratio (0.83) (Knicker et al., 2005); although the decrease was smaller than in the presence of O_2 (H/C 0.40). From the ^{13}C NMR results (Fig. C.1), it appears that the presence of O_2 preferentially reduced the contribution of the O-alkyl C, methoxyl and N-alkyl C, and alkyl C regions. Increasing charring duration intensified the contribution of the regions located at higher ppm (ketone C, carbonyl and amide C, O-aryl C and aryl and unsaturated C; Fig. C.2). At 425 °C, the presence of O_2 did not have a significant influence on the degree of aromatisation (Fig. 7), which suggests that at 425 °C a shorter duration of charring (6 h) was enough to achieve maximum condensation. Finally, BC formed at 600 °C (0.5 h) was even more aromatic when O_2 was present, but reached a plateau under full pyrolysis. Fig. 6 shows the increase in condensation when the charring duration was extended. This suggests a similar behaviour to the BC formed at 250 °C: short exposure to 600 °C was insufficient to reach maximum condensation but the presence of O_2 was able to compensate.

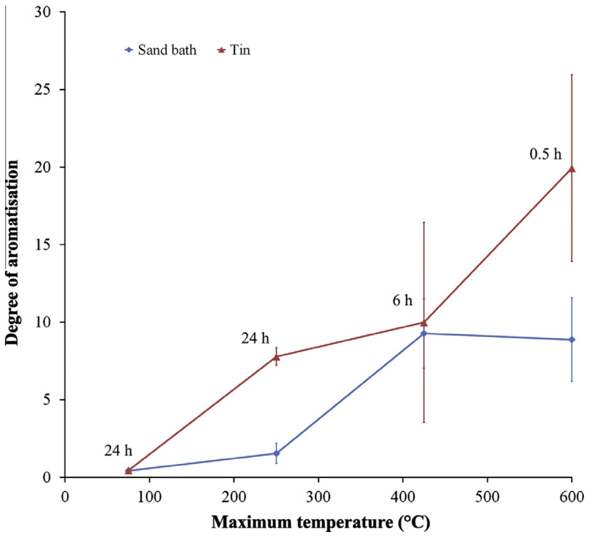

Fig. 7. Degree of aromatisation with increasing MT (75–600 °C) for BC formed under full (SB) or partial (Tin) pyrolysis conditions. The degree of aromatisation is the ratio of aromatic C to aliphatic and O-containing C [(165–110 ppm)/(110–0 ppm)]. Data are mean (± standard deviation). Charring duration (h) for each MT is specified.

4. Conclusions

Thermal treatment had a significant influence on both the chemical and physical properties of BC originating from various types of fuel. Results obtained for this reference set, produced under controlled thermal treatment, confirmed the importance of maximum temperature and fuel type as factors influencing the composition and physical properties of the resulting BC. Duration of charring and abundance of O_2 also influenced BC chemical properties.

As for the chemical properties, the type of fuel was most important for temperatures < 250–350 °C. Then, the main fuel components – cellulose, hemicelluloses and lignin – started to degrade and the maximum temperature became the dominant formation factor. Charring duration affected the composition at both low (250 °C) and high (⩾ 600 °C) temperature. The presence of O_2 affected BC composition mainly at low temperature, i.e. 250 °C, and resulted in accelerated alkyl C degradation. The H content and yield of BC were the two attributes most sensitive to other formation factors besides maximum temperature. With increasing temperature, we observed a decrease in yield, although at 250 °C, the presence of O_2 also provoked a drastic decrease in yield.

MT was the most influential factor with respect to physical properties. There was an important increase in BC porosity (specific surface area and total pore volume) with the more severe thermal treatments. Nevertheless, BC physical features appeared to also be under the control of the type of fuel.

Acknowledgments

The authors acknowledge the Natural Sciences and Engineering Research Council of Canada for a Strategic grant to A.D. Munson, S.A. Quideau, R.E. Wasylishen, R.L. Bradley, S.G. Cumming, S. Gauthier, D. Paré, and the Canadian Circumpolar Institute for a grant to L.S. R.W. thanks the University of Alberta and the Government of Canada for a Canada Research Chair in Physical Chemistry. We thank J. Liu and H. Campbell for laboratory assistance, the Integrated Nanosystems Research facility for access to the surface area analyzer, and N. Zhang for assistance. We acknowledge three anonymous reviewers for their time and effort in commenting on the manuscript.

Appendix A. Supplementary material

Supplementary data associated with this article can be found, in the online version, at http://dx.doi.org/10.1016/j.orggeochem.2013.07.005.

Associate Editor—**M. Simpson**

References

Antal, M.J., Grønli, M., 2003. The art, science, and technology of charcoal production. Industrial & Engineering Chemistry Research 42, 1619–1640.

ASTM, 2007. D1762-84 Standard Test Method for Chemical Analysis of Wood Charcoal. American Society for Testing and Materials International, West Conshohocken, PA.

Axelson, D.E., 2012. Solid State Nuclear Magnetic Resonance. A Practical Introduction, first ed. MRi_Consulting, Lexington, KY.

Baldock, J.A., Smernik, R.J., 2002. Chemical composition and bioavailability of thermally altered *Pinus resinosa* (Red pine) wood. Organic Geochemistry 33, 1093–1109.

Behar, F., Hatcher, P.G., 1995. Artificial coalification of a fossil wood from brown coal by confined system pyrolysis. Energy & Fuels 9, 984–994.

Belderok, H.J.M., 2007. Experimental Investigation and Modeling of the Pyrolysis of Biomass, MSc Thesis. Eindhoven University of Technology, Eindhoven, The Netherlands.

Bergeron, Y., Flannigan, M.D., 1995. Predicting the effects of climate change on fire frequency in the southeastern Canadian boreal forest. Water, Air and Soil Pollution 82, 437–444.

Bourke, J., Manley-Harris, M., Fushimi, C., Dowaki, K., Nunoura, T., Antal, M.J., 2007. Do all carbonized charcoals have the same chemical structure? 2. A Model of the chemical structure of carbonized charcoal. Industrial & Engineering Chemistry Research 46, 5954–5967.

Brown, R.A., Kercher, A.K., Nguyen, T.H., Nagle, D.C., Ball, W.P., 2006. Production and characterization of synthetic wood chars for use as surrogates for natural sorbents. Organic Geochemistry 37, 321–333.

Brunauer, S., Emmett, P.H., Teller, E., 1938. Adsorption of gases in multimolecular layers. Journal of the American Chemical Society 60, 309–319.

Calvelo Pereira, R., Kaal, J., Camps Arbestain, M., Pardo Lorenzo, R., Aitkenhead, W.P., Hedley, M., Macías, F., Hindmarsh, J., Maciá-Agulló, J.A., 2011. Contribution to characterisation of biochar to estimate the labile fraction of carbon. Organic Geochemistry 42, 1331–1342.

Certini, G., 2005. Effects of fire on properties of forest soils: a review. Oecologia 143, 1–10.

Chatterjee, S., Santos, F., Abiven, S., Itin, B., Stark, R.E., Bird, J.A., 2012. Elucidating the chemical structure of pyrogenic organic matter by combining magnetic resonance, mid-infrared spectroscopy and mass spectrometry. Organic Geochemistry 51, 35–44.

Degroot, W.F., Pan, W., Rahman, M.D., Richards, G.N., 1988. First chemical events in pyrolysis of wood. Journal of Analytical and Applied Pyrolysis 13, 221–231.

DeLuca, T.H., MacKenzie, M.D., Gundale, M.J., Holben, W.E., 2006. Wildfire-produced charcoal directly influences nitrogen cycling in Ponderosa pine forests. Soil Science Society of America Journal 70, 448–453.

Downie, A., Crosky, A., Munroe, P., 2009. Physical properties of biochar. In: Lehmann, J., Joseph, S. (Eds.), Biochar for Environmental Management: Science and Technology. Earthscan Publications Ltd., London, UK, pp. 13–32.

Earl, W.L., VanderHart, D.L., 1982. Measurement of ^{13}C chemical shifts in solids. Journal of Magnetic Resonance 48, 35–54.

Freitas, J.C.C., Bonagamba, T.J., Emmerich, F.G., 1999. ^{13}C high-resolution solid-state NMR study of peat carbonization. Energy & Fuels 13, 53–59.

Hammes, K., Smernik, R.J., Skjemstad, J.O., Herzog, A., Vogt, U.F., Schmidt, M.W.I., 2006. Synthesis and characterisation of laboratory-charred grass straw (*Oryza sativa*) and chestnut wood (*Castanea sativa*) as reference materials for black carbon quantification. Organic Geochemistry 37, 1629–1633.

Hammes, K., Schmidt, M.W.I., Smernik, R.J., Currie, L.A., Ball, W.P., Nguyen, T.H., Louchouarn, P., Houel, S., Gustafsson, Ö., Elmquist, M., Cornelissen, G., Skjemstad, J.O., Masiello, C.A., Song, J., Peng, P., Mitra, S., Dunn, J.C., Hatcher, P.G., Hockaday, W.C., Smith, D.M., Hartkopf-Fröder, C., Böhmer, A., Lüer, B., Huebert, B.J., Amelung, W., Brodowski, S., Huang, L., Zhang, W., Gschwend, P.M., Flores-Cervantes, D., Largeau, C., Rouzaud, J., Rumpel, C., Guggenberger, G., Kaiser, K., Rodionov, A., González-Vila, F.J., González-Pérez, J.A., De la Rosa, J.M., Manning, D.A.C., Lopez-Capél, E., Ding, L., 2007. Comparison of quantification methods to measure fire-derived (black/elemental) carbon in soils and sediments using reference materials from soil, water, sediment and the atmosphere. Global Biogeochemical Cycles 21, 2–18.

Han, X., Jiang, X., Yu, L., Cui, Z., 2006. Change of pore structure of oil shale particles during combustion. Part 1. Evolution mechanism. Energy & Fuels 20, 2408–2412.

Harden, J.W., O'Neill, K.P., Trumbore, S.E., Veldhuis, H., Stocks, B.J., 1997. Moss and soil contributions to the annual net carbon flux of a maturing boreal forest. Journal of Geophysical Research 102, 28805–28816.

Harden, J.W., Trumbore, S.E., Stocks, B.J., Hirsch, A., Gower, S.T., O'Neill, K.P., Kasischke, E.S., 2000. The role of fire in the boreal carbon budget. Global Change Biology 6, 174–184.

Harvey, O.R., Kuo, L., Zimmerman, A.R., Louchouarn, P., Amonette, J.E., Herbert, B.E., 2012. An index-based approach to assessing recalcitrance and soil carbon sequestration potential of engineered black carbons (biochars). Environmental Science & Technology 46, 1415–1421.

Hockaday, W.C., Grannas, A.M., Kim, S., Hatcher, P.G., 2006. Direct molecular evidence for the degradation and mobility of black carbon in soils from ultrahigh-resolution mass spectral analysis of dissolved organic matter from a fire-impacted forest soil. Organic Geochemistry 37, 501–510.

Hockaday, W.C., Grannas, A.M., Kim, S., Hatcher, P.G., 2007. The transformation and mobility of charcoal in a fire-impacted watershed. Geochimica et Cosmochimica Acta 71, 3432–3445.

Inari, G.N., Mounguengui, S., Dumarçay, S., Pétrissans, M., Gérardin, P., 2007. Evidence of char formation during wood heat treatment by mild pyrolysis. Polymer Degradation and Stability 92, 997–1002.

Kasischke, E.S., Stocks, B.J., 2000. Fire, Climate Change, and Carbon Cycling in the Boreal Forest, first ed. Springer-Verlag, New York.

Keiluweit, M., Nico, P.S., Johnson, M.G., Kleber, M., 2010. Dynamic molecular structure of plant biomass-derived black carbon (biochar). Environmental Science & Technology 44, 1247–1253.

Knicker, H., Totsche, K.U., Almendros, G., González-Vila, F.J., 2005. Condensation degree of burnt peat and plant residues and the reliability of solid-state VACP MAS ^{13}C NMR spectra obtained from pyrogenic humic material. Organic Geochemistry 36, 1359–1377.

Knicker, H., 2007. How does fire affect the nature and stability of soil organic nitrogen and carbon? A review. Biogeochemistry 85, 91–118.

Krull, E.S., Baldock, J.A., Skjemstad, J.O., Smernik, R.J., 2009. Characteristics of biochar – organo-chemical properties. In: Lehmann, J., Joseph, S. (Eds.), Biochar for Environmental Management: Science and Technology. Earthscan Publications Ltd., London, UK, pp. 53–66.

Lang, T., Jensen, A.D., Jensen, P.A., 2005. Retention of organic elements during solid fuel pyrolysis with emphasis on the peculiar behavior of nitrogen. Energy & Fuels 19, 1631–1643.

Lua, A.C., Yang, T., Guo, J., 2004. Effects of pyrolysis conditions on the properties of activated carbons prepared from pistachio-nut shells. Journal of Analytical and Applied Pyrolysis 72, 279–287.

Masiello, C.A., 2004. New directions in black carbon organic geochemistry. Marine Chemistry 92, 201–213.

Melkior, T., Jacob, S., Gerbaud, G., Hediger, S., Le Pape, L., Bonnefois, L., Bardet, M., 2012. NMR analysis of the transformation of wood constituents by torrefaction. Fuel 92, 271–280.

Miyanishi, K., 2001. Duff consumption. In: Johnson, E.A., Miyanishi, K. (Eds.), Forest Fires: Behavior & Ecological Effects. Academic Press, San Diego, pp. 437–475.

Orvis, K.H., Lane, C.S., Horn, S.P., 2005. Laboratory production of vouchered reference charcoal from small wood samples and non-woody plant tissues. Palynology 29, 1–11.

Peersen, O.B., Wu, X.L., Kustanovich, I., Smith, S.O., 1993. Variable-amplitude cross-polarization MAS NMR. Journal of Magnetic Resonance, Series A 104, 334–339.

Ponomarenko, E.V., Anderson, D.W., 2001. Importance of charred organic matter in Black Chernozem soils of Saskatchewan. Canadian Journal of Soil Science 81, 285–297.

Preston, C.M., Schmidt, M.W.I., 2006. Black (pyrogenic) carbon in boreal forests: a synthesis of current knowledge and uncertainties. Biogeosciences 3, 397–420.

Rein, G., Cleaver, N., Ashton, C., Pironi, P., Torero, J.L., 2008. The severity of smouldering peat fires and damage to the forest soil. Catena 74, 304–309.

Ryan, K.C., 2002. Dynamic interactions between forest structure and fire behavior in boreal ecosystems. Silva Fennica 36, 13–39.

Schlesinger, W.H., Bernhardt, E.S., 2013. The global carbon cycle. In: Schlesinger, W.H., Bernhardt, E.S. (Eds.), Biogeochemistry – An Analysis of Global Change. Academic Press, Boston, pp. 419–444.

Schmidt, M.W.I., Noack, A.G., 2000. Black carbon in soils and sediments: analysis, distribution, implications, and current challenges. Global Biogeochemical Cycles 14, 777–793.

Schmidt, M.W.I., Skjemstad, J.O., Gehrt, E., Kögel-Knabner, I., 1999. Charred organic carbon in German chernozemic soils. European Journal of Soil Science 50, 351–365.

Sing, K.S.W., Everett, D.H., Haul, R.A.W., Moscou, L., Pierotti, R.A., Rouquérol, J., Siemieniewska, T., 1985. Reporting physisorption data for gas/solid systems with special reference to the determination of SA and porosity (Recommendations 1984). Pure and Applied Chemistry 57, 603–619.

Sivonen, H., Maunu, S.L., Sundholm, F., Jämsä, S., Viitaniem, P., 2005. Magnetic resonance studies of thermally modified wood. Holzforschung 56, 648–654.

Skjemstad, J.O., Reicosky, D.C., Wilts, A.R., McGowan, J.A., 2002. Charcoal carbon in U.S. agricultural soils. Soil Science Society of America Journal 66, 1249–1255.

Smernik, R.J., Oades, J.M., 2000a. The use of spin counting for determining quantitation in solid state ^{13}C NMR spectra of natural organic matter: 1. Model systems and the effects of paramagnetic impurities. Geoderma 96, 101–129.

Smernik, R.J., Oades, J.M., 2000b. The use of spin counting for determining quantitation in solid state ^{13}C NMR spectra of natural organic matter: 2. HF-treated soil fractions. Geoderma 96, 159–171.

Smernik, R.J., Baldock, J.A., Oades, J.M., Whittaker, A.K., 2002. Determination of $T_1\rho^H$ relaxation rates in charred and uncharred wood and consequences for NMR quantitation. Solid State Nuclear Magnetic Resonance 22, 50–70.

Taylor, S.W., Wotton, B.M., Alexander, M.E., Dalrymple, G.N., 2004. Variation in wind and crown fire behaviour in a northern jack pine – black spruce forest. Canadian Journal of Forest Research 34, 1561–1576.

Wardle, D.A., Zackrisson, O., Nilsson, M., 1998. The charcoal effect in boreal forests: mechanisms and ecological consequences. Oecologia 115, 419–426.

Wikberg, H., Maunu, S.L., 2004. Characterisation of thermally modified hard- and softwoods by ^{13}C CPMAS NMR. Carbohydrate Polymers 58, 461–466.

Yu, Z., Apps, M.J., Bhatti, J.S., 2002. Implications of floristic and environmental variation for carbon cycle dynamics in boreal forest ecosystems of central Canada. Journal of Vegetation Science 13, 327–340.

Zackrisson, O., Nilsson, M., Wardle, D.A., 1996. Key ecological function of charcoal from wildfire in the boreal forest. Oikos 77, 10–19.

Zimmerman, A.R., 2010. Abiotic and microbial oxidation of laboratory-produced black carbon (biochar). Environmental Science & Technology 44, 1295–1301.